

Structural and magnetic properties of L1₀-FePd/MgO films on GaAs and InP lattice mismatched substrates

M. Kohda, S. Iimori, R. Ohsugi, H. Naganuma, T. Miyazaki, Y. Ando, and J. Nitta

Citation: *Appl. Phys. Lett.* **102**, 102411 (2013);

View online: <https://doi.org/10.1063/1.4795443>

View Table of Contents: <http://aip.scitation.org/toc/apl/102/10>

Published by the [American Institute of Physics](#)

Articles you may be interested in

[L1₀ ordered phase formation in FePt, FePd, CoPt, and CoPd alloy thin films epitaxially grown on MgO\(001\) single-crystal substrates](#)

Journal of Applied Physics **111**, 07A708 (2012); 10.1063/1.3672856

[Structure and magnetic properties of FePd-alloy epitaxial thin films grown on MgO single-crystal substrates with different orientations](#)

Journal of Applied Physics **109**, 07B757 (2011); 10.1063/1.3563038

[Growth of L1₀-ordered crystal in FePt and FePd thin films on MgO\(001\) substrate](#)

AIP Advances **6**, 085302 (2016); 10.1063/1.4960554

[Controlling microstructure and magnetization process of FePd \(001\) films by staged thermal modification](#)

Applied Physics Letters **95**, 172503 (2009); 10.1063/1.3246795

[Influence of stoichiometry and growth temperature on the crystal structure and magnetic properties of epitaxial L1₀ Fe-Pd \(001\) films](#)

Journal of Applied Physics **115**, 17A740 (2014); 10.1063/1.4867229

[Effect of a change in thickness on the structural and perpendicular magnetic properties of L1₀ ordered FePd ultra-thin films with \(001\) texture](#)

Journal of Applied Physics **112**, 113919 (2012); 10.1063/1.4769737

Scilight

Sharp, quick summaries **illuminating**
the latest physics research

Sign up for **FREE!**

AIP
Publishing

Structural and magnetic properties of $L1_0$ -FePd/MgO films on GaAs and InP lattice mismatched substrates

M. Kohda,^{1,2} S. Iimori,¹ R. Ohsugi,¹ H. Naganuma,³ T. Miyazaki,⁴ Y. Ando,³ and J. Nitta¹

¹Department of Materials Science, Tohoku University, Sendai 980-8579, Japan

²PRESTO, Japan Science and Technology Agency, Kawaguchi 332-0012, Japan

³Department of Applied Physics, Tohoku University, Sendai 980-8579, Japan

⁴Department of Instrumental Analysis, Tohoku University, Sendai 980-8579, Japan

(Received 30 January 2013; accepted 28 February 2013; published online 13 March 2013)

Structural and magnetic properties of epitaxial $L1_0$ -FePd/MgO films on GaAs and InP lattice mismatched substrates are investigated at different MgO and FePd growth temperatures. While c -axis lattice constants of MgO and FePd show similar values on both substrates, the remanent magnetization becomes larger on GaAs than that on InP. Since the ratio of FePd (002) tetragonal ordered phase and FePd (200) cubic disordered phase follows similar growth temperature dependence to the remanent magnetization and the long range chemical order parameter, the perpendicular magnetic anisotropy grown on the lattice-mismatched semiconductors is strongly affected by formation of the disordered phase. © 2013 American Institute of Physics.

[<http://dx.doi.org/10.1063/1.4795443>]

In the field of spintronics, a ferromagnet (FM)/semiconductor (SC) hybrid structure has attracted increasing interest for electrical spin injection and detection^{1,2} as well as magneto-optical effect.^{3,4} Widely studied FM/SC structures, such as Fe, CoFe, and (Ga,Mn)As grown on GaAs substrate,^{5–8} usually employ magnetic easy axis along an in-plane direction. These structures have demonstrated spin light emitting diode operation and electrical spin injection/detection in non-local device geometry.^{1,2,5–8} However, for future spintronic devices combined with magneto-optical interaction⁴ and spin manipulation,⁹ a perpendicularly magnetized FM/SC structure is indispensable.

Chemically ordered ($L1_0$) FePd exhibits large perpendicular magnetic anisotropy of the order of 10^7 erg/cm³ (Refs. 10 and 11) and high magneto-optical response.^{12,13} In addition, an $L1_0$ -FePd thin film can be grown on an MgO layer which also acts as a tunnel barrier for an efficient spin injection. Hence, the $L1_0$ -FePd/MgO/semiconductor structure will be a promising candidate for spin-based electronic and optical devices. For semiconductor materials, GaAs/AlGaAs and InP/InGaAs heterostructures are widely used for high electron mobility transistors and telecommunication devices because of small effective mass and direct band gap materials, which will enable us to realize the threshold reduction of a vertical cavity surface emitting laser⁸ and a reconfigurable logic circuit¹⁴ based on spin degree of freedom. However, GaAs and InP substrates exhibit large lattice mismatch to the $L1_0$ -FePd and MgO films. In previous studies, while we have grown $L1_0$ -FePd/MgO films on GaAs,^{15,16} the crystallographic origin for degrading the remanent magnetization and the long range chemical order parameter has not been understood. By comparing structural and magnetic properties of $L1_0$ -FePd grown on different lattice-mismatched substrates, we can clarify the crystallographic origin affecting on the perpendicular anisotropy in $L1_0$ -based FM/SC hybrid structures.

In this letter, we sputtered 20 nm $L1_0$ -FePd/10 nm MgO films on GaAs and InP substrates at different MgO and FePd

growth temperatures and investigated the structural and magnetic properties. The growth temperatures were varied from room temperature (RT) to 400 °C for MgO and from 300 °C to 500 °C for $L1_0$ -FePd, respectively. For both growth conditions, MgO and FePd lattice constants exhibited similar values on GaAs and InP substrates. However, the ratio of remanent magnetization to saturation magnetization for the $L1_0$ -FePd showed higher values on GaAs than that on InP. By analyzing X-ray diffraction (XRD) patterns, we revealed that the ratio of FePd (002) tetragonal ordered phase and FePd (200) cubic disordered phase shows similar growth temperature dependence to the remanent magnetization as well as a long range chemical order parameter, which can explain the crystallographic origin affecting on the perpendicular magnetic anisotropy in an $L1_0$ -based FM/MgO/SC system.

$L1_0$ -FePd and MgO films are grown on GaAs (001) and InP (001) substrates in an ultrahigh vacuum magnetron sputtering system. Prior to the sputtering, a surface oxidized layer is removed by chemical etching with 35% hydrofluoric acid (HF) for 1 min followed by 1 min rinse with deionized water. The surface roughness after the HF etching is as small as 0.252 nm measured by atomic force microscopy (AFM). The etched wafers are immediately transferred to the sputtering chamber to avoid the surface oxidization and are annealed at 400 °C for 20 min for surface cleaning. The growth rate of MgO and $L1_0$ -FePd films are 0.065 Å/s (Ar pressure 0.1 Pa) and 0.114 Å/s (Ar pressure 0.6 Pa), respectively. In order to compare the structural and magnetic properties of 20 nm $L1_0$ -FePd/10 nm MgO films on lattice-mismatched substrates, 10-mm-square wafers of GaAs and InP are prepared on a single substrate holder and simultaneous sputtering is performed. $L1_0$ -FePd/MgO films are grown at different MgO and FePd temperatures, T_S (MgO) and T_S (FePd). For present studies, two sets of samples are prepared: First set is T_S (MgO) = RT, 200 °C, 300 °C, and 400 °C with T_S (FePd) = 300 °C, and second set is T_S (FePd) = 300 °C, 400 °C, and 500 °C with T_S (MgO) = 300 °C. All FePd films

are covered with 4 nm-thick Ta as a capping layer. The structural, surface, and magnetic characterizations are carried out by XRD, cross sectional transmission microscopy (TEM), AFM, and polar magneto-optical Kerr effect (PMOKE).

Since the lattice mismatch between MgO and GaAs (InP) shows over 25%, which could affect the perpendicular magnetic anisotropy, we first investigate the MgO growth temperature dependence at T_S (FePd) = 300 °C. Figures 1(a) and 1(b) show the XRD results for $L1_0$ -FePd/MgO films on GaAs and InP substrates, respectively. In the case of GaAs substrate, clear MgO (002) peaks are observed at all T_S (MgO), which brings about the epitaxial growth of an $L1_0$ -FePd as confirmed by FePd (002) fundamental peak as well as FePd (001) super lattice peak. However, for the InP substrate, an MgO (002) peak and an $L1_0$ -FePd phase are only observed at T_S (MgO) = 200 °C and 300 °C, suggesting that the MgO crystallinity is affected by different lattice mismatched substrates. In previous study, we have confirmed the crystallographic relationship between MgO and GaAs as MgO (001) || GaAs (001) along the growth direction.¹⁵ In order to figure out the InP case, we carry out the TEM observation for the sample sputtered at T_S (MgO) = 300 °C. Figures 2(a) and 2(b) show the cross-sectional TEM images of the $L1_0$ -FePd/MgO/InP structure and Figs. 2(c) and 2(d) exhibit the nano-beam electron diffraction (NBD) patterns along (1–10) direction in the InP region and in the MgO/InP interface region, respectively. The high resolution TEM image shown in Fig. 2(b) reveals the flat interfaces at the InP/MgO and MgO/ $L1_0$ -FePd, which becomes the advantage for efficient electrical spin injection. While the lateral crystallite diameter of the MgO is on the order of a few 10 nm due to the large lattice mismatch between MgO and InP substrate, $L1_0$ -FePd shows small dispersion of c -axis crystal orientation resulting in the larger crystallite diameter on the order of a few 100 nm. In Figs. 2(c) and 2(d), we observed

the ordered spot patterns and, by comparing dashed yellow and blue lines in the NBD patterns, the reflections from the InP and MgO films are identified as MgO (001) || InP (001) crystallographic relationship. As a result, the MgO (001) film shows the cube-on-cube epitaxial relationship also for the InP (001) substrate. Figure 1(c) shows the c -axis lattice constants of the MgO and FePd films with different T_S (MgO) evaluated from XRD results. While the MgO lattice constant is slightly changed between 0.421 and 0.418 nm, the similar lattice constant is obtained for the MgO film grown on GaAs and InP. The c -axis lattice constants of the $L1_0$ -FePd on GaAs and InP become smaller values than bulk FePd (0.372 nm), indicating a tensile strain induced by the MgO film. Although the MgO lattice constant shows weak temperature dependence, there is almost no substrate difference both for the MgO and $L1_0$ -FePd lattice constants.

For further optimizing the structural properties of the $L1_0$ -FePd, we next investigate the FePd growth temperature dependence. We set T_S (MgO) = 300 °C because of the clear observation of MgO (002) peak both on GaAs and InP substrates. Figures 1(d)–1(f) show XRD results and evaluated c -axis lattice constants. For both GaAs and InP substrates, FePd (002) fundamental peak as well as FePd (001) super lattice peak are observed at all T_S (FePd) due to optimized MgO crystallinity. Since the $L1_0$ -FePd lattice constants are almost same between GaAs and InP substrates, similar crystallographic properties are obtained in the $L1_0$ -FePd/MgO films on GaAs and InP substrates.

In order to investigate magnetic property of the $L1_0$ -FePd film, we next carry out a PMOKE measurement by applying a perpendicular external magnetic field to the film plane. Figures 3(a)–3(d) show the out-of-plane magnetic field dependence of normalized PMOKE signals for the $L1_0$ -FePd on GaAs and InP substrates at different MgO and FePd growth temperatures. The observed hysteresis of

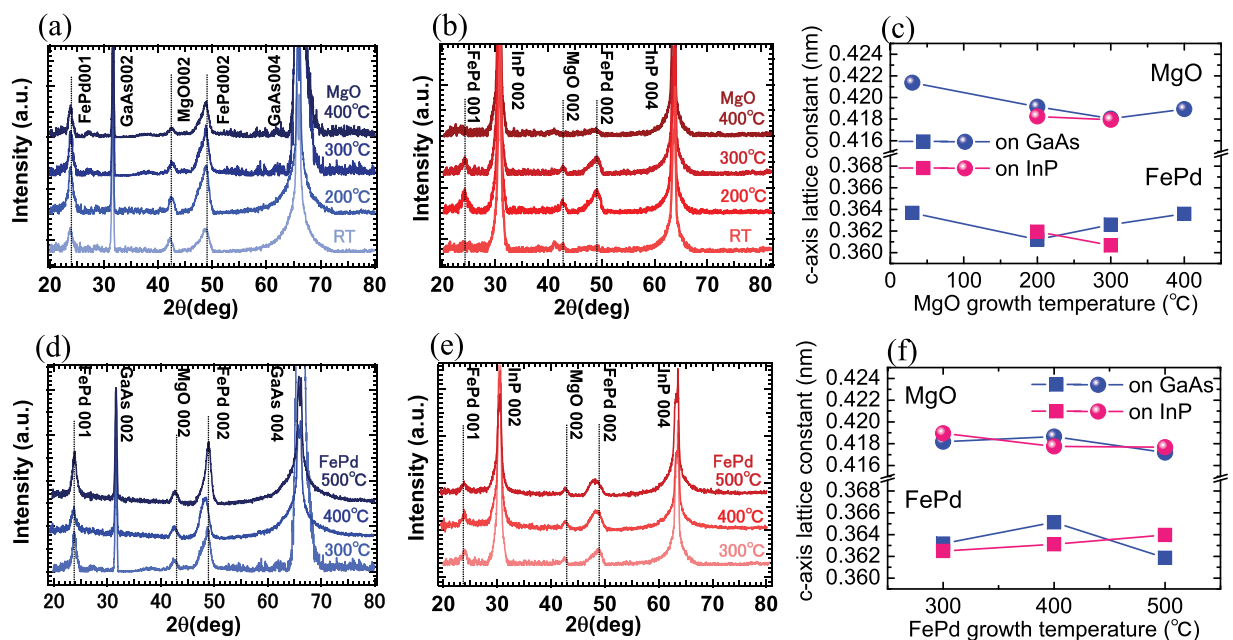


FIG. 1. XRD patterns and lattice constants of MgO and FePd in different growth temperature conditions. XRD patterns of different MgO growth temperature on (a) GaAs and (b) InP and (c) evaluated c -axis lattice constant from XRD measurement. XRD patterns of different FePd growth temperature on (d) GaAs and (e) InP and (f) c -axis lattice constant.

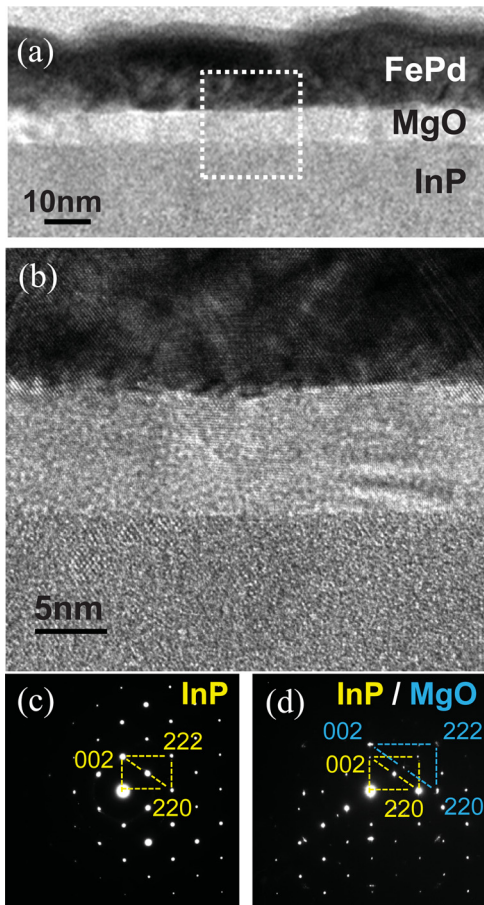


FIG. 2. (a) Cross-sectional TEM image. (b) High resolution TEM image. The selected area corresponds to the dotted square region in (a). Nano beam diffraction patterns taken from (c) InP layer and from (d) MgO/InP interface.

$L1_0$ -FePd on GaAs shows better squareness and larger coercivity than that on InP. As shown in Figs. 3(e) and 3(f), the ratio of remanent magnetization to saturation magnetization (M_r/M_s) exhibits clear temperature dependence both for GaAs and InP substrates. Despite the similar lattice constants of the $L1_0$ -FePd and MgO films on GaAs and InP substrates, much higher M_r/M_s is obtained for the $L1_0$ -FePd on GaAs than that on InP. In order to explain the difference of M_r/M_s , we first focus on the FePd (001) super lattice peak in the growth condition of T_S (MgO) = 300 °C and T_S (FePd) = 500 °C. As shown in Fig. 4(a), full-width at half maximum (FWHM) of the FePd (001) on InP shows 1.187°, while the FWHM on GaAs becomes narrower value of 0.897°. Similar FWHM dependence is also observed in different MgO growth temperatures. Since both peaks are well fitted by a single Lorentz function (Black lines in Fig. 4(a)), such a difference indicates that the distortion of the MgO c -axis from the perpendicular direction depends on the lattice mismatched substrates, which influences on the structural and magnetic properties of $L1_0$ -FePd. To further investigate the MgO lattice distorted effect to the $L1_0$ -FePd structural properties, we next compared FePd (002) fundamental peaks on GaAs and InP as shown in Figs. 4(b) and 4(c). The dotted and dashed lines correspond to the calculated peak position of FePd (002) and FePd (200). Unlike the FePd (001) peaks in Fig. 4(a), two different peaks are superimposed near the

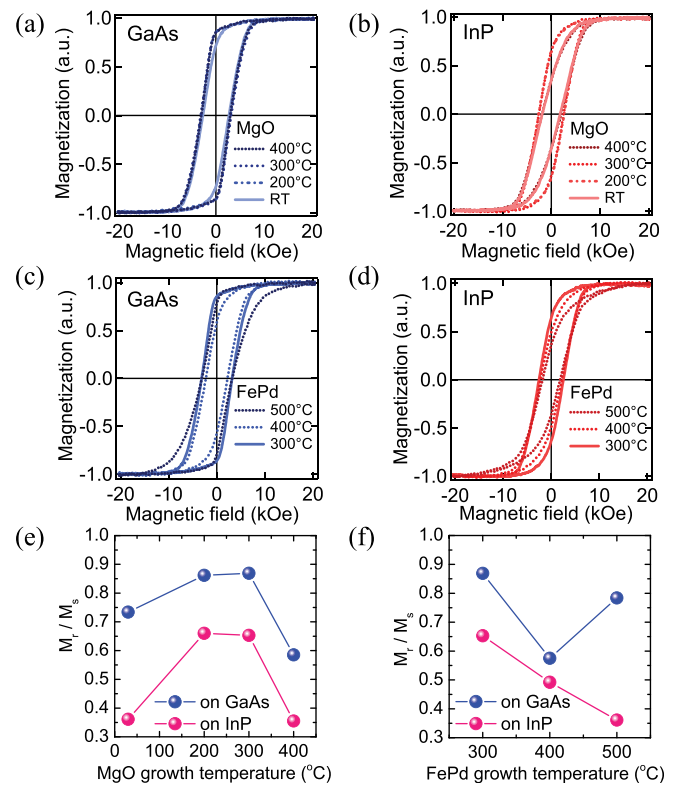


FIG. 3. Magnetic field dependence of normalized PMOKE signals for different MgO temperature on (a) GaAs and (b) InP and for different FePd temperature on (c) GaAs and (d) InP. The ratio of remanent magnetization to saturation magnetization (M_r/M_s) as a function of (e) MgO and (f) FePd growth temperatures.

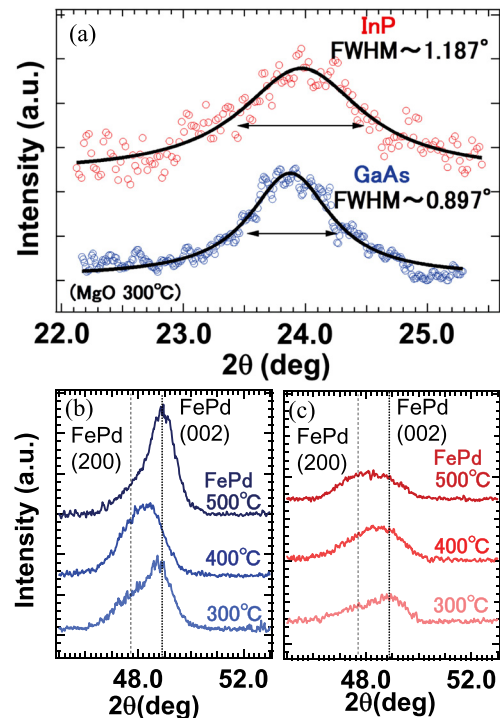


FIG. 4. (a) FePd (001) super lattice peaks grown on GaAs and InP at T_S (MgO) = 300 °C. Black lines are the fitting with single Lorentz function. FePd (002) fundamental peaks for different growth temperatures on (b) GaAs and (c) InP.

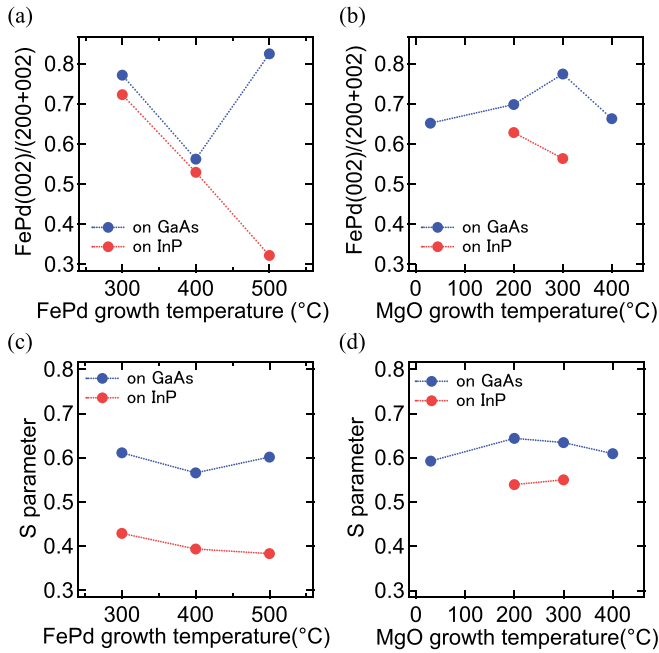


FIG. 5. The ratio of FePd (002) tetragonal ordered phase and FePd (002) + FePd (200) phases as a function of (a) FePd and (b) MgO growth temperatures. The long range chemical order parameter S as a function of (c) FePd and (d) MgO growth temperatures.

FePd (002) fundamental peak position. The second peak is located at lower angle, indicating the coexistence of FePd (002) tetragonal ordered phase and FePd (200) cubic disordered phase. In order to estimate the ratio of these two phases, we extract the relative areas of FePd (002) and FePd (200) diffraction patterns by fitting two Lorentz functions. Figures 5(a) and 5(b) show the ratio between the FePd (002) ordered phase and the FePd (002) + FePd(200) phases as a function of FePd and MgO growth temperatures. In all samples, the ratio of the FePd (002) tetragonal ordered phase is higher for the $L1_0$ -FePd on GaAs than that on InP. It is noted that the ratio of the FePd (002) tetragonal ordered phase follows similar temperature dependence to M_r/M_s in Figs. 3(e) and 3(f). Since the remanent magnetization of the disordered phase is aligned in an in-plane, the increase of the disordered phase decreases the remanent magnetization. As a result, the temperature dependence of M_r/M_s is explained by the formation of the FePd (200) cubic disordered phase. Finally, we extracted the long range chemical order parameter S in Figs. 5(c) and 5(d). While $S \sim 0.6$ is constantly obtained for the $L1_0$ -FePd on GaAs in different growth temperatures, S for the $L1_0$ -FePd on InP reduces to 0.38–0.55. The temperature dependence of S parameter follows Figs. 5(a) and 5(b), suggesting that the formation of the FePd (200) cubic disordered phase affects both on the M_r/M_s and the S parameter for $L1_0$ -FePd grown on GaAs and InP. Since the cubic disordered phase is also observed in different $L1_0$ -based materials grown on GaAs substrate and reduces the M_r/M_s ,¹⁶ reduction of the cubic disordered phase would be a key to achieve the larger perpendicular magnetic anisotropy on semiconductor substrates.

Difference of the FePd (200) cubic disordered phase formation between GaAs and InP substrates might be due to the lattice periodicity between MgO and GaAs(InP). The in-plane lattice length of three GaAs unit cells corresponds to

the length scale of four MgO unit cells with 0.44% lattice mismatch, which could suppress the c -axis distortion during the MgO growth. However, an InP unit cell does not hold such a relationship to an MgO lattice constant. As can be seen in Fig. 2(a), the misfit dislocations are observed from the interface of the FePd/MgO. Such a dislocation of the FePd film enhances the FePd (200) cubic disordered phase during the growth, resulting in the degradation of remanent magnetization on InP in comparison with GaAs substrate.

In conclusion, we have investigated structural and magnetic properties of the $L1_0$ -FePd/MgO films on GaAs and InP lattice mismatched substrates by changing the MgO and FePd growth temperatures. While the lattice constants of the MgO and $L1_0$ -FePd on GaAs and InP shows the similar values, the M_r/M_s ratio exhibits clear temperature dependence both for GaAs and InP and becomes much larger values for the $L1_0$ -FePd on GaAs than that on InP. This temperature dependence is explained by the relative ratio between the FePd (002) tetragonal ordered phase and the FePd (200) cubic disordered phase. Since the temperature variation of long range chemical order parameter S also follows to the disordered phase ratio, suppression of the cubic disordered phase becomes important for the perpendicularly magnetized FM/SC hybrid structures.

We thank Professor Seki and Professor Takanashi for PMOKE measurement and useful discussions. This work was supported in part by Grant for Advanced Industrial Technology Development from NEDO, by the Japan Science and Technology Agency (JST) through its Strategic International Cooperative Program under the title “Advanced spintronic materials and transport phenomena (ASPIMATT)” and by the Mayekawa Foundation.

- ¹Y. Ohno, D. K. Young, B. Beschoten, F. Matsukura, H. Ohno, and D. D. Awschalom, *Nature* **402**, 790 (1999).
- ²X. Lou, C. Adelmann, S. A. Crooker, E. S. Garlid, J. Zhang, K. S. M. Reddy, S. D. Flexner, C. J. Palmström, and P. A. Crowell, *Nat. Phys.* **3**, 197 (2007).
- ³W. Zaets and K. Ando, *IEEE Technol. Lett.* **11**, 1012 (1999).
- ⁴H. Shimizu and Y. Nakano, *Jpn. J. Appl. Phys., Part 2* **43**, L1561 (2004).
- ⁵M. Kohda, T. Kita, Y. Ohno, F. Matsukura, and H. Ohno, *Appl. Phys. Lett.* **89**, 012103 (2006).
- ⁶X. Lou, C. Adelmann, M. Furis, S. A. Crooker, C. J. Palmström, and P. A. Crowell, *Phys. Rev. Lett.* **96**, 176603 (2006).
- ⁷I. Appelbaum, B. Huang, and D. J. Monsma, *Nature* **447**, 295 (2007).
- ⁸M. Holub, J. Shin, D. Saha, and P. Bhattacharya, *Phys. Rev. Lett.* **98**, 146603 (2007).
- ⁹J. Nitta, T. Akazaki, H. Takayanagi, and T. Enoki, *Phys. Rev. Lett.* **78**, 1335 (1997).
- ¹⁰N. Miyata, H. Asami, T. Mizushima, and K. Sato, *J. Phys. Soc. Jpn.* **59**, 1817 (1990).
- ¹¹T. Seki, T. Shima, K. Takanashi, Y. Takahashi, E. Matsubara, and K. Hono, *Appl. Phys. Lett.* **82**, 2461 (2003).
- ¹²G. Armelles, D. Weller, B. Rellinghous, P. Caro, A. Cebollada, and F. Briones, *J. Appl. Phys.* **82**, 4449 (1997).
- ¹³K. Takayama, T. Sugimoto, Y. Suzuki, M. Hashimoto, P. De Haan, and J. C. Lodder, *J. Mag. Magn. Mater.* **104**, 1002 (1992).
- ¹⁴Y. Kunihashi, M. Kohda, H. Sanada, H. Gotoh, and T. Sogawa, *Appl. Phys. Lett.* **100**, 113502 (2012).
- ¹⁵M. Kohda, A. Ohtsu, T. Seki, A. Fujita, J. Nitta, S. Mitani, and K. Takanashi, *Jpn. J. Appl. Phys., Part 1* **47**, 3269 (2008).
- ¹⁶R. Ohsugi, M. Kohda, T. Seki, A. Ohtsu, M. Mizuguchi, K. Takanashi, and J. Nitta, *Jpn. J. Appl. Phys., Part 1* **51**, 02BM05 (2012).